Fractional quantum Hall effect in second subband of a 2DES

A Letters Journal Exploring the Frontiers of Physics

May 2011

EPL, **94** (2011) 37010
doi: 10.1209/0295-5075/94/37010

www.epljournal.org

Fractional quantum Hall effect in second subband of a 2DES

C. A. Duarte[1(a)], L. E. G. Armas[2], E. C. F. da Silva[3], G. M. Gusev[3], A. K. Bakarov[4], S. Wiedmann[5] and J. C. Portal[5,6,7]

[1] *Departamento de Física, Universidade Federal do Paraná - CP 19044, CEP 81531-990, Curitiba, PR, Brazil*
[2] *Instituto de Física, Universidade Federal de Alagoas - 57072-970, Alagoas, Brasil*
[3] *Instituto de Física da Universidade de São Paulo - CP 66318, CEP 05315-970, São Paulo, SP, Brazil*
[4] *Institute of Semiconductor Physics - Novosibirsk, 630090, Russia*
[5] *GHMFL-CNRS - BP-166, F-38042 Grenoble Cedex 9, France, EU*
[6] *INSA-Toulouse - F-31077 Toulouse Cedex 4, France, EU*
[7] *Institut Universitaire de France - Toulouse, France, EU*

received 25 November 2010; accepted in final form 26 March 2011
published online 27 April 2011

PACS 71.30.+h – Metal-insulator transitions and other electronic transitions
PACS 73.40.Qv – Metal-insulator-semiconductor structures (including semiconductor-to-insulator)

Abstract – In the present paper we report on the experimental electron sheet density *vs.* magnetic field diagram for the magnetoresistance R_{xx} of a two-dimensional electron system (2DES) with two occupied subbands. For magnetic fields above 9 T, we found fractional quantum Hall levels centered around the filing factor $\nu = 3/2$ in both the two occupied electric subbands. We focused specially on the fractional levels of the second subband, whose experimental values of the magnetic field B of their minima do not obey a periodicity law in $1/|B - B_c|$, where B_c is the critical field at the filling factor $\nu = 3/2$, and we explain this fact entirely in the framework of the composite fermions theory. We use a simple theoretical model to give a possible explanation for the fact.

Introduction. – The study of high-electron-mobility semiconductor nanostructures at low temperatures and at high magnetic fields has revealed a variety of new phenomena associated to energy quantization in magnetic field and to many-body effects. One of the very known ones is the integer quantum Hall effect (IQHE), which is a consequence of the quantization of the electron energy levels in the sequence of Landau levels (LL).

The IQHE consists in the appearance of a series of plateaux in the transversal magnetoresistance R_{xy} (Hall resistance), acompanied by a series of minima in the longitudinal magnetoresistance R_{xx} [1]. In the IQHE the positions of these R_{xy} plateaux and R_{xx} and minima are determined by the values of the filling factor ν, which must fit integer values. At yet higher mobilities, a new effect emerges whose origin lies on electron many-body interactions. It is manifested by similar features on both R_{xx} and R_{xy}, and is well known as fractional quantum Hall effect (FQHE) [2], since the plateaux (minima) in R_{xy} (R_{xx}) appear at fractional values of the filling factor ν. The early investigations have shown that in the FQHE $\nu = p/(2p+1)$ with $p > 1$ and $\nu = p/(2p-1)$ with $p \geqslant 1$.

In order to give a theoretical explanation for the FQHE, the concept of composite fermions (CF) [3] has been postulated, in a framework where both IQHE and FQHE are described in a unified picture. In this theoretical model, the FQHE of electrons is considered to be equivalent to the IQHE of CF. To explain the fractional values of the filling factor ν, it is assumed that each electron is coupled to an even number n of quanta of magnetic flux $\phi_0 = h/2e$ (usually n being equal to 2), which is equivalent to say that each electron is coupled to a fraction of a quantum of magnetic flux ϕ_0/n. As a consequence of this coupling, the external magnetic B field is reduced by the amount $B_c = n_s\phi_0$, where n_s is the electron sheet density, and the residual magnetic field is given by $|B - B_c|$. In particular, the recent observation of the fractional state at $\nu = 5/2$ [4] led to consider the existence of even-denominator filling factors that are known as non-Abelian states that could have implications in quantum computation [5].

Recently the appearance was reported of fractional levels of two distinct electric subbands in a series of magnetoresistance spectra [6]. In the present work we will concentrate our attention on the fractional states around the $\nu = 3/2$ states belonging to the second electric subband in a AlGaAs/GaAs triple quantum well (TQW).

(a) E-mail: celso@fisica.ufpr.br

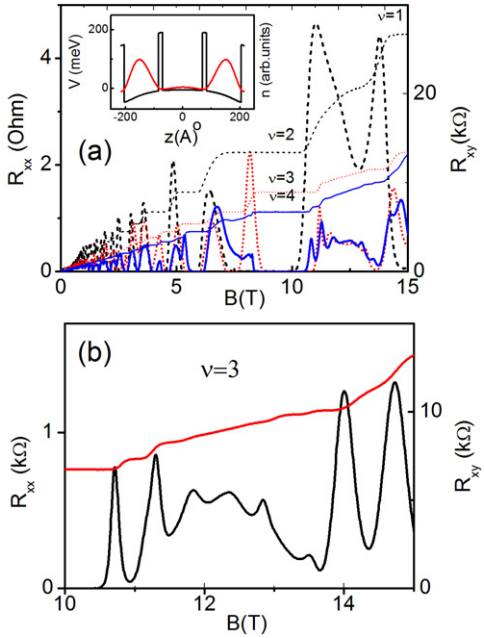

Fig. 1: (Color online) (a) Single-trace SdH and Hall spectra of the TQW sample R121, at different gate voltages: $-2.0\,\mathrm{V}$ (dashed black lines), $-1.25\,\mathrm{V}$ (dotted red lines) and $0.0\,\mathrm{V}$ (solid blue lines). Some filling factors are shown. (b) Enlarged view of the spectrum shown in (a) corresponding to zero gate voltage. The filling factor $\nu = 3$ is marked. The insert of (a) shows the calculated electron-density profile (dashed curve) and conduction-band edge E_c (solid curve) at zero gate voltage, when we have an electron density ($n_s = 9.0 \times 10^{11}\,\mathrm{cm}^2$).

In fig. 1(a) we present the result of Shubnikov-de Haas (SdH) and Hall measurements on our triple quantum well (TQW) sample R121 for different applied gate voltages V_g. It can be seen the wide quantum Hall plateaux in the Hall resistivity, acompanied by the vanishing of longitudinal magnetoresistance R_{xx}. At fields between 10 T and 15 T it can be seen a series of oscillations in R_{xx} that reveals the emergence of fractional quantum Hall states, which disappear with the application of large negative voltages. In fig. 1(b) we present an enlarged view of these fractional states for the case of $V_g = 0.0\,\mathrm{V}$. It can be clearly seen the disappearance of the plateau at filling factor $\nu = 3$ for $V_g = 0.0\,\mathrm{V}$, which gives place to the emergence of fractional levels at $\nu = 1 + 3/2$, that soften as a negative voltage is applied (see fig. 1(a)).

This work is organized as follows: in the second section we present the details of the samples and of the measurements. The third section is dedicated to present the experimental results and the analysis of the experimental data, and the fourth section summarizes the conclusions of this work.

Samples and experimental details. – Two samples of TQW and one sample of double quantum well (DQW) were grown on undoped (100) GaAs substrates by molecular-beam epitaxy. The DQW system comprises two 140 Å thick GaAs wells separated by a 14 Å wide $Al_{0.3}\,Ga_{0.7}As$ barrier. In the TQW structures, the central well (140 Å wide) is wider than the side wells (120 Å wide) in order to the Coulomb electron repulsion do not completely deplete the central well, allowing electron tunneling between the lateral wells. The barriers between the wells were 14 Å wide (sample R120) and 20 Å wide (sample R121) of undoped $Al_{0.3}Ga_{0.7}As$ layers. In all samples, carriers are supplied by two Si remote delta doping layers (nominal doping concentration in each Si layer $2.2 \times 10^{11}\,\mathrm{cm}^{-2}$) located on both sides of the structures.

Shubnikov-de Haas (SdH) and Hall measurements were performed on the samples on the Hall bar geometry at the temperature of 50 mK in a bath cryostat inserted into a superconducting coil using standard lock-in techniques. The test samples have 100 μm wide Hall bars with the distance between the voltage probes $L = 200\,\mu$m. The ohmic contacts were made with In. An evaporated Ti/Au frontside gate was used to control the electron densities within the layers. We measured the longitudinal and Hall resistivities varying the applied gate voltage V_g with steps of 0.02 V in the range from $-1.5\,\mathrm{V}$ to $+1.0\,\mathrm{V}$ for the DQW sample, from $-2.5\,\mathrm{V}$ to $+0.76\,\mathrm{V}$ for the TQW sample R120 and from $-1.2\,\mathrm{V}$ to $0.8\,\mathrm{V}$ for the TQW sample R121, sweeping the external magnetic field from 0 to 15 T, applied perpendicularly to the two-dimensional electron layers. The applied current was typically about 1 μA.

Experimental results. – Transport measurements revealed that the TQW samples R120 and R121 showed fractional levels (FQHE) more distinctly seen than the DQW sample in the studied range of magnetic fields and gate voltages. However, sample R121 showed the best mobility and as a consequence the minima in R_{xx} at the fractional levels region are more pronounced. By this reason this work will focus on the results of this sample.

SdH spectra for sample R121 were grouped in a colourmap, which corresponds to the diagram of R_{xx} in the plane $n_s \times B$ shown in fig. 2(a). In this diagram we clearly see a series of parallelogramlike structures resulting from the crossing of magnetoresistance peaks, and one of these parallelograms is involved by a dotted circumference in the figure. Both parallelogramlike and ringlike structures have been reported as a characteristic of two subband occupancy in 2DES [7–9], and their origin lies on the particular behavior of the Fermi energy as a function of the magnetic field. While the ringlike structures are typical for two occupied subband single-layer systems [7–9], the parallelograms seem most likely to resemble the magnetoresistance of two independent systems with different electron densities. In fact, in fig. 2(a) the magnetoresistance peaks form two series of lines: the first, a set of almost vertical parallel straight lines, which is associated to a 2DES with constant electron density (since the period in $1/B$ does not vary with n_s) and correspond to the LLs of the first electric subband;

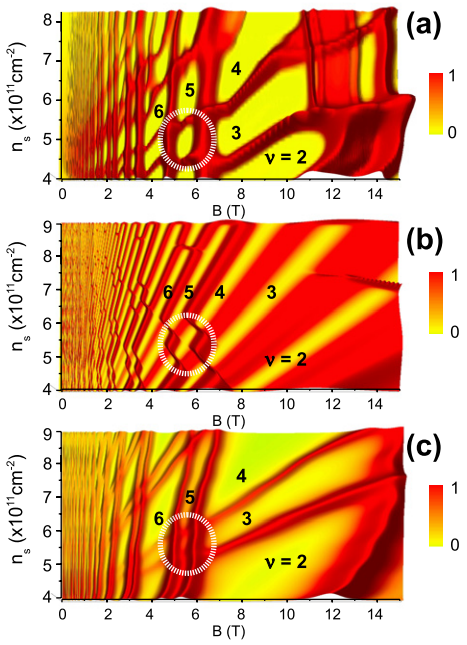

Fig. 2: (Color online) (a) Experimental colourmap of the magnetoresistance R_{xx} for the TQW sample R121. (b) Corresponding simulated colourmap without phenomenological smoothing ($\mu = 1$) and (c) with smoothing ($\mu = 0.5$). In all these three colourmaps, some filling factors are shown and the parallelogramlike structures that have correspondence in the colourmaps are stressed by the dotted circle (see explanation on the text).

and the second, a set of inclined lines, which is associated to a 2DES with increasing electron density (since the period in $1/B$ increases with n_s), and corresponds to the LLs of the second electric subband. Actually the two 2DEGs are not independent in sample R121, since neither the inclined lines nor the vertical ones are perfect straight lines, revealing some intersubband charge transfer which is a clear consequence of the expected electron tunneling along the central well. In particular, while the sample R121 showed typically parallelogramlike structures, the sample R120 showed ringlike ones (we will not present the colourmap for this sample since this comparison of shape of structures is not the main purpose of this article, and this study can be found elsewhere). Note that the internal barriers between the three wells in sample R121 (20 Å wide) are wider than the barriers on sample R120 (14 Å wide), so the lower value of barrier width increases the tunneling in sample R120, increasing the mutual dependence of the electron populations confined on the two occupied subbands of sample R120.

In fig. 2(b) we present a R_{xx} colormap diagram obtained by a numerical simulation using a single-particle theoretical model for the magnetoresistance [9]. The fitting parameters were chosen in order to achieve the best similarity to the experimental diagram for sample R121 (fig. 2(a)): the GaAs electron effective mass $m^* = 0.066m_e$ and the Landé g-factor -0.44 enhanced by an exchange contribution with $\alpha = 0.1$ [9,10]; also, the symmetric-antisymmetric energy gap Δ_{SAS} [11], whose value showed to be almost linearly dependent on the total electron sheet density n_s, such that from $n_s = 6.5 \times 10^{11}\,\mathrm{cm}^{-2}$ to $10 \times 10^{11}\,\mathrm{cm}^{-2}$, Δ_{SAS} varied from 7.3 meV to zero. The inspection of figs. 2(a) and (b) reveals that the vertical lines in panel (a) are not present in panel (b), in place of what we see "zigzag" shaped lines. For magnetic fields in the range between 2.5 and 4.0 T and n_s in the range between 5.5 and $7.0 \times 10^{11}\,\mathrm{cm}^{-2}$ the experimental colourmap of fig. 2(a) is slightly different from the calculated one shown in fig. 2(b) probably because of the emergence of some LLs belonging to the third subband.

According to the above considerations concerning the ringlike and parallelogramlike structures present in the $n_s \times B$ magnetoresistance diagrams, it is clear that to avoid the "zigzag" shape and achieve better similarity between calculated and the experimental diagrams it is necessary to eliminate or at least reduce the charge transfer between the two lowest occupied subbands. Avoiding more elaborate self-consistent calculations to determine the electron distribution within the TQW in the presence of external magnetic field B, we simply applied a simple phenomenological smoothing on the Fermi energy[1],

$$E_F(B) \to E_F(0) + \mu\,[E_F(B) - E_F(0)], \qquad (1)$$

where μ is an arbitrary parameter. This smoothing does not change our conclusions and will be useful in the further analysis of the fractional states. In fact, the shape of the Fermi energy is decisive for the determination of the morphology of the magnetoresistance $n_s \times B$ diagrams [12], but we must stress here that such a phenomenological smoothing does not modify the topology of the $n_s \times B$ diagrams neither with respect to the IQHE levels nor with respect to the FQHE levels. In fact, we repeated the calculation without the smoothing process (not presented here for brevity) and confirmed that all the conclusions that we achieved to in this work are the same. In fig. 2(c) we present a simulation with smoothed Fermi energy with $\mu = 0.5$. The strong similarity between the theoretical smoothed (see fig. 2(c)) and experimental (see fig. 2(a)) results ensures the convenience of the smoothing procedure. Note that the "zigzag" lines found in the simulated colourmap of fig. 2(b) are converted in almost straight lines in fig. 2(c). Yet in this figure we enclosured with a dotted circle the same parallelogram that corresponds to the structures evidenced in figs. 2(a) and (b).

Let us go back to the experimental colourmap, fig. 2(a). Above around 10 T, we can see the onset of the emergence of fractional levels which are seen enlarged in fig. 3(a). In this figure, around $n_s = 5.8 \times 10^{11}\,\mathrm{cm}^{-2}$ some fractional levels centered about the field $B_{c1} = 13$ T emerge as a

[1]In fact, in our calculations we considered that subband energy separations Δ_{SAS} are constant with respect to the magnetic field, but in a more elaborated model where the Schrödinger and Poisson equations are solved self-consistently for nonzero magnetic field, they do not necessarily result constant.

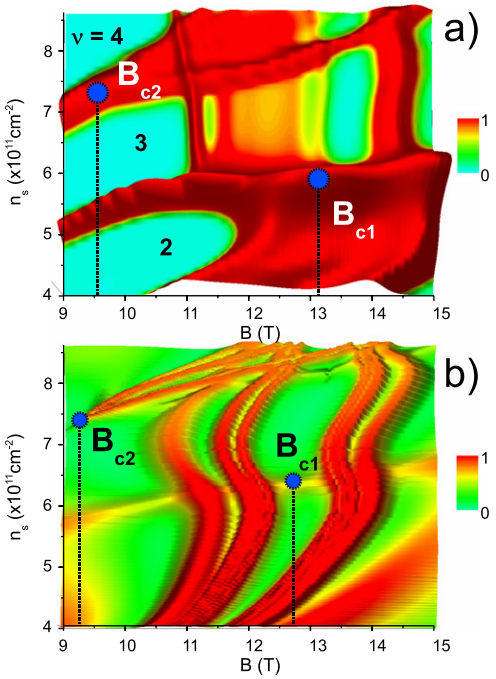

Fig. 3: (Color online) (a) Detail of the $n_s \times B$ diagrams of sample R121 shown in fig. 2(a), where we can see clearly the onset of the formation of the fractional states of the first (vertical dashed lines) and the second (inclinated dashed lines) populated electric subband levels. Some of the fractional as well as integer filling factors are marked. (b) A numerically simulated diagram with the best fitting parameters for comparison.

set of almost vertical lines, which we will label as F_1. Similarly, another set emerges centered around the field $B_{c2} = 9.9\,\mathrm{T}$ when $n_s = 7.5 \times 10^{11}\,\mathrm{cm}^{-2}$, which we will label as F_2. A particular detail that can be seen after inspection of fig. 3(a) is the fact that crossing of the sets F_1 and F_2 do not show the above-mentioned ringlike structures. Following our above considerations, we can conclude that there is not a CF interchange between both these fractional states F_1 and F_2.

The unexpected convergence of the lines of the set F_2 to the point at B_{c2} has the most profound implication that the values of the magnetic field B of the minima of the levels in F_2 do not follow a periodicity in $1/|B - B_{c2}|$, which is a very known characteristic typical of LL in the FQHE regime. In other words, for a given value of the total electron density n_s, the positions of the minima of the magnetoresistance R_{xx} in the fractional region of the second subband cannot be calculated uniquely by this $1/|B - B_{c2}|$ rule, since the fractions positions are primarily determined by their filling factors $\nu_2 = p/(2p \pm 1)$ (see the first section) and the mathematical relation between B and ν_2 involves the second subband electron sheet density, $\nu_2 = n_{s,2}/|B - B_{c2}|$.

In fig. 3(b) we show for comparison a simple simulated diagram with the same fitting parameters of fig. 2(c) employing the theoretical model described in the appendix. For simplicity, we do not consider the contribution of electrons arisen from delocalized states. Important assumptions in this calculations were the following:

1) CF and electrons were considered as independent particles, in the sense that they have independent Fermi energies[2];

2) The intersubband energy separation between the CF Landau fans is not itself Δ_{SAS}, but a lower value (we have employed for simplicity the value $1/2\Delta_{SAS}$) —which is essential to give the convergence of the set F_1 to a point (B_{c2}).

In addition, we have considered that the CF effective mass is given by [2]

$$m^* = \beta m_0 \sqrt{B}, \tag{2}$$

where m_0 is the electron rest mass and β is a parameter with units of $B^{-1/2}$ [14]. We verified that this parameter determines the position of the point B_{c2} in the colourmap. Our fitting yeilded $\beta = 0.2\,\mathrm{T}^{-1/2}$, a value that was previously reported [14]. In this simulation we show only low-order fractional levels ($p_{1,2} = 1$, 2, 3 in the expression $\nu_i = p_i/(2p_i \pm 1)$).

In the calculations within our model, we verified that below B_{c2} there is another set of fractions around $\nu_2 = 1 + 1/2$ that emerge (in other words, B_{c2} is a "quenching point" for the fractional set F_2). However, we are not interested on this low-field region since we do not see any fraction in the experimental colormap of fig. 3(b) below B_{c2}.

Note that the upper regions of the colormap of figs. 3(a) and (b) extend up to $n_s = 8.6 \times 10^{11}\,\mathrm{cm}^{-2}$, the same as in the experimental colormap of fig. 2(a). Unfortunately this limits the visualization of the crossing region that could be benefited if we extended the upper limit to higher n_s value. However, note that we are treating the crossing of fractions around the same value of subband filling factor, *i.e.*, $\nu_1 = \nu_2 = 1 + 1/2$, which in the limit when ν_1 crosses ν_2 there are equal subband populations, $n_{s,1} = n_{s,2}$, since in this case the symmetric-antisymmetric gap Δ_{SAS} vanishes. Then, any higher value of total n_s must correspond to constant zero Δ_{SAS}, and as a consequence the color map does not present crossings and new topology above $n_s = 8.6 \times 10^{11}\,\mathrm{cm}^{-2}$.

The set of fractional levels belonging to the first subband that appear in the experimental plot of fig. 3(a) are neither straight lines nor vertical in the simulated diagram of fig. 3(b). However, this morphological dissimilarity does not represent any topological difference between the experimental results and our simple model and within the limitations of our calculation model it is acceptable.

Finally, it is worth noting that the positions of the minima of fractional states are not determined by the value of the effective mass of CF (parameter β), neither

[2]In fact, this is valid for the case of one single occupied subband, as we verified and as can be find in previous work [13].

by the fact that the CF cyclotron frequency ω_{CF,L_i} has a peculiar dependence on the square root of the field (see eq. (A.6)).

Conclusion. – We studied the LL crossing between the fractional levels belonging to different subbands at double occupancy. Using a simple theoretical model based on the CF theory, we could construct a calculated colormap of the magnetoresistance with a topology similar to that of the experimental colormap. Also, we verified that the crossings between fractional levels belonging to the two occupied electric subbands do not show ringlike structures.

* * *

Support of this work by FAPESP and CNPq (Brazilian funding agencies) is acknowledged.

Appendix: theoretical fitting of the magnetoresistance at fractional levels. – Here we present the theoretical model for our calculations. The basic assumption is that each magnetoresistance peak is associated to the coincidence of the Fermi level E_F with an energy level of the system —either associated to IQH or FQH. The value of R_{xx} is obtained by the inversion of the conductivity tensor $\widetilde{\sigma}$, where the longitudinal conductivity σ_{xx} is calculated by the Kubo formula [9].

The problem starts with the determination of the function density of states $DOS(E)$ that depends explicitly on the energy E and implicitly on the magnetic field B. As we have determined $DOS(E)$, we must solve the equation

$$n_s = \int_{-\infty}^{E_F(B)} DOS\,(B,E)\,\mathrm{d}E \tag{A.1}$$

from which we determine the explicit dependence of the Fermi energy $E_F(B)$ on the magnetic field B.

Starting from the expression for the DOS in the case of the IQH [9], our generalization for the DOS for a 2DEG that includes both integer and fractional quantum Hall levels in the ideal zero-temperature case is given by

$$DOS(E) = \sum_{\{n\}} \zeta_n \delta_n(E), \tag{A.2}$$

where the summation is carried out on all the available energy levels (integer and fractional) labeled by n. In this expression, ζ_n is the level degeneracy of the n-th energy level, and $\delta_n(E)$ the corresponding functional density (as will be explained later). For the IQH levels, ζ_n is independent of the order n of the level and is given simply by $\zeta = eB/h$, a well-known result. On the other side, for the fractional levels the degeneracy depends on the level and can be calculated simply by means of the filling factor ν [15]. The degeneracy of the fractional level at filling factor $\nu = p/(2p \pm 1)$ is $\zeta_p = \nu/(\nu - L)\zeta = \nu/(\nu - L)eB/h$. However, the net magnetic field B_{net} experienced by the CF is not equal to the total applied magnetic field B, and this must be considered on this expression for ζ_p. For example, it can be shown that at the fractional level $\nu = 3/2$ the net field is given by $B_{net} = 3(B - B_{3/2})$, where $B_{3/2}$ is the value of the magnetic field at $\nu = 3/2 = 1 + 1/2$ [15]. Generalizing this expression for any fractional level p around $L + 1/2$, where $L = 0, 1, \ldots$ labels the Landau level index, we obtain $B_{net} = 2\nu(B - B_{L+1/2})$. Then, the complete expression for the fractional level degeneracy is

$$\zeta_p = \frac{\nu}{\nu - L} \frac{e\,(2L+1)\,\left|B - B_{L+1/2}\right|}{h}. \tag{A.3}$$

Without loss of generality the level functional density of states $\delta_n(E)$ was chosen to be a Lorentzian [9,16],

$$\delta_n = \frac{\Gamma}{1 + (\frac{E_n - E}{\Gamma})^2}, \tag{A.4}$$

where Γ is the level broadening. In our calculations, we used a level broadening $\Gamma = h/\tau_q$ independent of the magnetic field [9], but we used different quantum lifetimes τ_q for electrons (at IQH levels) and CF (at fractional levels). The fitted values for the broadening parameters do not necessarily correspond to the expected from experiment since in our approximation we did not consider the delocalized states. For the IQH levels, the label n in expression (A.4) represents the set of numbers $\{L, i, s\}$, where $i = 1, 2, \ldots$ is the subband index and $s = \pm 1$ labels the spin. The energy levels in the IQH regime are given by

$$E_{L,i,s} = \left(L + \frac{1}{2}\right) \hbar\omega_c + \Delta_i + 1/2 s g^* \mu_B B, \tag{A.5}$$

where $\omega_c = eB/m^*$ is the electron cyclotron frequency, Δ_i is subband energy and the last term contains the Zeeman and exchange spin contributions [10,17]. In our notation, for the first subband level $i = 1$, $\Delta_1 = 0$ and Δ_2 coincides with the well-known symmetric-antisymmetric energy gap Δ_{SAS}. The situation for the FQH is similar, as we need only to consider that the LL energy fan for CF is generated by an effective cyclotron frequency

$$\omega_{CF} = \frac{e\,|B - B_c|}{\beta m^* \sqrt{B}}. \tag{A.6}$$

Neglecting the spin contribution of CF, the energy spectrum for the FQHE is

$$E_{l,i} = \left(p_i + \frac{1}{2}\right) \hbar\omega_{CF,L_i} + (L_i - 1/2)\,\hbar\omega_c\,(B_{c,i}) + \Delta_i, \tag{A.7}$$

where the lower-case p_i labels the fractional level of the i-th subband, the upper-case L_i labels the integer LL index corresponding to the $\nu_i = L_i + 1/2$ fractional level. The second term $(L_i - 1/2)\hbar\omega_c(B_{c,i})$ is an essential offset energy, whose explanation will be presented later. Labeling the CF cyclotron frequency ω_{CF,L_i} by the index L_i, it is

given by

$$\omega_{CF,L_i} = \frac{e\,|B - B_c|}{\beta m_e \sqrt{B}} = \frac{e2\nu\,\left|B - B_{L_1+1/2}\right|}{\beta m_e \sqrt{B}} \tag{A.8}$$

as we conclude from our above considerations. Then, the FQHE contribution to expression (A.2) is

$$\sum_{p,i} \zeta_{p,i}\delta_{p,i}(E) = \sum_{p,\pm} \frac{\nu_{p,\pm}}{\nu_{p,\pm} - L_i} \frac{2e\nu\left(B - B_{L_i+1/2}\right)}{h} \times \frac{\Gamma}{1 + (\frac{E_{p,i}-E}{\Gamma})^2}, \tag{A.9}$$

where $\nu_{p,\pm} = L + p/(2p \pm 1)$ is the filling factor of the CF level labeled by the integer p.

An important parameter is the effective CF field B_c. The theory previews that B_c originates from the CF system, acting in opposition to the external applied field B, and B_c coincides with the value of B at the filling factor $\nu_i = L_i + 1/2$. In practice, calculations need the determination of this filed. Since $\nu = n_s e/hB$,

$$B_{c,i} = \frac{n_{s,i}e}{h(L_i + \frac{1}{2})}, \tag{A.10}$$

then, $B_{c,i}$ depends on the electron density on the i-th subband, $n_{s,i}$, obtained by

$$n_{s,i} = \int_{\infty}^{E_F(B)} DOS_i\,(E)\,\mathrm{d}E, \tag{A.11}$$

where $DOS_i(E)$ means the sum of terms of the DOS associated to the integer and fractional levels of the i-th subband.

The complete procedure of calculation is the following: we start solving eq. (A.1) considering a density of states function $DOS(B, E)$ comprising the totality of *integer* levels and *none* of the fractionals; then, we determine E_F and in sequence the individual subband electron sheet densities $n_{s,i}$ solving the eq. (A.11). Immediately we determine the values of the fields $B_{c,i}$ with eq. (A.10). After that, we reconstruct the $DOS(B, E)$ function with fractional and integer states. Particularlly, now including all the integer levels *except for* the integer level L_i at filling factor $\nu_i = L_i + 1/2$ that will be further substituted by the sum of the fractional states. In other words, we keep the IQHE DOS and replace the subband i integer level at $\nu_i = L_i + 1/2$ by the sum of fractional states (centered at ν_i). In sequence, we determine the IQHE+FQHE Fermi energy solving eq. (A.1). Then, the longitudinal conductivity σ_{xx} is calculated using Kubo's formula

$$\sigma_{xx} = \sum_{\{n\}} \lambda_n \delta_n^*(B), \tag{A.12}$$

where for the integer levels $\lambda_n = (L_i + 1/2)e^2/h$. For $\delta_n^*(B)$ we used [9]

$$\delta_n^*(B) = \frac{1}{1 + 2(\frac{E_n - E_F(B)}{\Gamma})^2}. \tag{A.13}$$

For the fractional levels, until our knowledge there is not an expression for σ_{xx}. Despite this fact, in this qualitative approach we can in principle try any value for λ_n, for what we used a phenomenological value $\lambda = 0.5$, which gave good fitting to experimental data. Having the longitudinal conductivity of the system IQH+FQH, we determine the longitudinal resistivity ρ_{xx} component of the resistivity tensor from which we determine the desired magnetoresistance R_{xx} [9].

An important detail is the following. Solving eq. (A.1), we verify that the average value of $E_F(B)$ in the IQH region is much higher than the average values in the FQHE region. Constructing both the Landau fans of the IQHE and the FQHE in the same diagram together with $E_F(B)$ (*i.e.*, the IQHE fan centered on the zero magnetic field and zero energy point, and the FQHE fans centered on $B_{c,i}$ and zero energy points), we verify that levels of the FQHE fans will cross the Fermi level in the region of IQH. This would represent the appearance of unphysical fractional peaks in the region of pure IQH. This problem is solved adding a positive offset value to the CF energy. As was done in eq. (A.7), the most sensate choice for this offset is the value of the electron cyclotron energy at the field $B_{c,i}$.

REFERENCES

[1] Klitzing K., *Phys. Rev. Lett.*, **45** (1980) 494.
[2] Halperin B. I., Patrick A. Lee and Nicholas Read, *Phys. Rev. B*, **47** (1993) 7312.
[3] Jain J., *Composite Fermions* (Cambridge University Press) 2007.
[4] Willet R., Eisenstein J. P., Störmer H. L., Tsui D. C., Gossard A. C. and English J. E., *Phys. Rev. Lett.*, **59** (1987) 1776.
[5] Nayak C., Simon S. H., Stern A., Freedman M. and Das Sarma S., *Rev. Mod. Phys.*, **80** (2008) 1083.
[6] Shabani J. and Shayegan M., arXiv:1004.0979 [cond-mat.mes-hall], 6 April 2010.
[7] Zhang X. C., Faulhaber D. R. and Jiang H. W., *Phys. Rev. Lett.*, **95** (2005) 216801.
[8] Ellenberger C., Simovič B., Letureq R., Ihn T., Ulloa S. E., Ensslin K., Driscoll D. C. and Gossard A. C., *Phys. Rev. B*, **74** (2006) 195313.
[9] Duarte C. A., Gusev G. M., Quivy A. A., Lamas T. E., Bakarov A. K. and Portal J. C., *Phys. Rev. B*, **76** (2007) 75346.
[10] Leadley D. R., Nicholas R. J., Harris J. J. and Foxon C. T., *Phys. Rev. B*, **58** (1998) 13036.
[11] Gusev G. M., Duarte C. A., Lamas T. E., Bakarov A. K. and Portal J. C., *Phys. Rev. B*, **78** (2008) 155320.
[12] Davies A. G., Barnes C. H. W., Zolleis K. R., Nicholls J. T., Simmons M. Y. and Ritchie D. A., *Phys. Rev. B*, **54** (1996) R17331.
[13] Dial O. E., Ashoori R. C., Pfeiffer L. N. and West K. W., *Nature*, **464** (2010) 566.
[14] Schulze-Wischeler F., Mariani E., Hohls F. and Haug R. J., *Phys. Rev. Lett.*, **92** (2004) 156401.
[15] Ihn T., *Semiconductor Nanostructures* (Oxford University Press) 2010.
[16] Zhang X. C., Martin I. and Jiang H. W., *Phys. Rev. B*, **74** (2006) 73301.
[17] Fogler M. M. and Shklovskii B. I., *Phys. Rev. B*, **52** (1995) 17366.